

SWIRL-SWITCHING PHENOMENON IN TURBULENT FLOW THROUGH TOROIDAL PIPES

Azad Noorani

Swedish e-Science Research Centre (SeRC)
Linné FLOW Centre, KTH Mechanics
SE-100 44 Stockholm, Sweden
azad@mech.kth.se

Philipp Schlatter

Swedish e-Science Research Centre (SeRC)
Linné FLOW Centre, KTH Mechanics
SE-100 44 Stockholm, Sweden
pschlatt@mech.kth.se

ABSTRACT

Direct numerical simulations (DNS) are performed to investigate turbulent flows in toroidal pipes with mild and strong curvature. By means of proper orthogonal decomposition (POD), dominant structures in the flow field are identified. The most energetic structures in the strongly curved pipes ($\kappa = 0.1$ and $\kappa = 0.3$) are very similar in both configurations studied here. These modes (shape and frequency) also match the coherent structures responsible for swirl switching phenomenon found earlier in experimental and numerical studies of turbulent flow in spatially developing 90° bends with which the current results are compared. The observed swirl switching in toroidal pipes, which is isolated from any upstream and separation conditions, may challenge the current hypothesis regarding the origin of swirl switching mechanism.

INTRODUCTION

Turbulent flow in curved pipes is widely occurring in a variety of industrial applications. Heat and mass transfer systems such as heat exchangers, chemical reactors and pipeline systems are obvious examples. The imbalance between the cross-stream pressure gradient and geometry induced centrifugal forces in curved pipes results in a secondary circulation. This leads to the formation of a pair of counter-rotating vortices, so-called Dean vortices, which force the streamwise velocity to be distributed non-uniformly in the cross-section of the pipe. The strength of these Dean cells (*i.e.* the magnitude of the secondary motion in bent pipes) is controlled by two parameters; namely, the bulk Reynolds number of the flow and the curvature of the bend. In this article the bulk Reynolds number is defined as $Re = u_b D / \nu$; based on the bulk velocity u_b , pipe diameter D and kinematic viscosity ν . The nondimensionalised curvature parameter κ , is defined as $\kappa = R_a / R_c$; R_a being the radius of a generic cross-section of the pipe and R_c is the radius of curvature at the pipe centreline. This parameter (κ) distinguishes between mild curvature ($\kappa \approx 0.01$) and strong curvature ($\kappa \gg 0.01$).

Spatially developing bends such as 90° bends and helically coiled tubes are two distinct variants of curved pipe geometries. While fully developed flow from a straight pipe enters the bend in the former category, the flow is fully developed inside the curve in the latter geometry. Ignoring the effect of the pitch in helically coiled pipes is a reasonable assumption (as holds for most practical applications) which simplifies the geometry to that of a toroidal pipe. Such an infinitely long bent pipe configuration provides a unique opportunity to isolate the effect of the curvature on the turbulent characteristics and also to study the influence of the centrifugal forces and the secondary motion on the near-wall features. Notwithstanding, both spatial bends and toroidal configurations share similar characteristics inside the curved geometry. In this article *pipe-bends* are referred to as spatially developing bends, and *continuously curved pipes* means toroidal pipes.

The complexity of the flow field in curved pipe configurations made it difficult to unfold the intrinsic dynamics related to the turbulent flow in toroidal pipes. Noorani *et al.* (2013) recently performed DNSs of turbulent flow in straight, mildly curved and strongly continuously bent pipes. These authors computed the Reynolds stress budgets for various curvature configurations and identified the effect of the curvature on the near-wall dynamics of turbulent flow.

To date, the interaction of near-wall turbulence with Dean vortices has remained unclear. While these vortex cells are symmetric with respect to the plane of symmetry of the pipe in the mean flow, it seems they exhibit an oscillatory behaviour instantaneously. Tunstall & Harvey (1968) who performed experimental flow visualisations in a mitred bend ($\kappa \rightarrow \infty$) by injecting talc and dye in turbulent flow of air (at $Re = 217000$) and water (at 40000) observed that instead of a classical twin Dean cells, the secondary motion was dominated by a single vortex (swirl) that abruptly switches the rotation between clockwise (CW) and counter-clockwise (CCW) with a low frequency. This bi-stable state of the secondary motion is known as swirl switching. The Strouhal number ($St = fD/u_b$, where f de-

notes the frequency) associated with the mean frequency of the swirl switching was found to be 0.002 by Tunstall & Harvey (1968). They suggested that the two stable configurations of single cells, which are mirror images of each other, are characterized by the inner-corner separation region being displaced into an asymmetric position. They also speculated that the switching of the circulation to the opposite sense could be due to sufficiently large turbulent eddies with opposing circulation entering the bend. According to Tunstall & Harvey (1968) the necessary conditions for swirl switching are the separation at the inner bend position (*i.e.* acute enough bend to force separation) and high Reynolds number turbulent flow in circular pipes.

Thirty years later, with developing particle image velocimetry (PIV) technique, Brücker (1998) visualised the unsteady behaviour of the Dean cells downstream of a 90° bend with $\kappa = 0.5$ at $Re = 2000$ and 5000 by considering isosurfaces of planar vorticity. Assessing a spatio-temporal diagram of the these isosurfaces (computed with Taylor hypothesis) revealed the alternating domination of Dean cells. Correspondingly, the plane of symmetry of this twin vortex was oscillating about the symmetry plane of the bend. Analyzing the power spectral density (PSD) of the tangential velocity at the bend symmetry plane shows that this is a quasi-periodic phenomenon which is dominated by two distinct Strouhal numbers, 0.03 and 0.12.

This research was continued by Rütten *et al.* (2001, 2005) by means of large eddy simulations (LES) of the flow in spatially developing bends with $\kappa = 0.5$ and 0.17 at $Re = 5000 - 27000$. These studies confirmed the alternating domination of Dean cells observed by Brücker (1998). The PSD analysis of the total force over the pipe wall after the bend in streamwise and tangential directions revealed a series of low- and high-frequencies on the order of $St \approx 0.01$ and $St = 0.2 - 0.3$. They suggested that the low frequency is due to the swirl switching. These authors also computed the instantaneous stagnation point of the Dean cells in the outer bend by low-pass filtering of the velocity field. The low frequency determined from the PSD of the peripheral orientation of this stagnation point appears to agree with the low-frequency force exertion at the wall.

Proper orthogonal decomposition (POD) technique was first used by Sakakibara *et al.* (2010) to analyse swirl switching using the PIV measurements of the turbulent flow at multiple points downstream of a pipe-bend with $\kappa = 0.75$ at $Re = 120000$. While the first POD mode resembles a single swirl spanning the entire pipe section, by reconstructing the flow field with mean flow and the most energetic POD structures, they could observe the alternating domination of the Dean cells close to the bend. These modes also operated at a low frequency of $St = 0.07$.

Sakakibara & Machida (2012) also used PIV data of an experimental set up with $\kappa = 0.5$ and $Re = 27000$ to identify the stagnation point of Dean vortices in the inner- and the outer-bend positions. Unlike Rütten *et al.* (2005), from the measurements of Sakakibara & Machida (2012) it appears that the Dean cells' stagnation point at the outer bend fluctuates randomly in the azimuthal direction of the pipe. On the other hand, the more regular fluctuations of this stagnation point in the inner bend considered to represent the swirl switching motion. The linear stochastic estimation of the conditional velocity is applied to the field upstream of the bend and resulted in identifying high- and low-speed streaky structures with lengths comparable to the very large scale motion (VLSM) introduced by Kim & Adrian (1999).

According to Sakakibara & Machida (2012) these VLSM like structures are responsible for the switching mechanism.

Other experimental and numerical investigations of Hellström *et al.* (2013), Kalpakli Vester *et al.* (2015) and Carlsson (2014) were also conducted to link the VLSM to swirl switching. Similar to Sakakibara *et al.* (2010), Hellström *et al.* (2013) performed PIV on a flow at multiple positions downstream of the bend with $\kappa = 0.5$ and $Re = 25000$. Applying POD to the in-plane velocity data and reconstructing the flow field with most energetic structures combined with the Taylor hypothesis shows the movement and the resilience of this alternating domination of the Dean cells downstream of the bend. While the most energetic POD mode in this study also resembles the single swirl motion identified by Sakakibara *et al.* (2010), the frequency associated with the temporal evolution of this mode is surprisingly higher than what was found in the previous studies under similar conditions.

Kalpakli Vester *et al.* (2015) also tried to control the swirl switching mechanism by mounting a honeycomb inside the pipe upstream of the bend with $\kappa = 0.39$ at $Re = 23000$. This resulted in a severe change of the flow downstream of the bend in the sense that the mean Dean cells and the single-vortex structure did not appear in their POD analysis of the data obtained adjacent to the bend. However, these structures appeared in the POD analysis of the flow at further downstream.

In the current study, DNSs of turbulence in infinitely long toroidal pipes with various curvatures are performed. In this way the effect of the curvature on the near-wall turbulence is isolated *i.e.* no separation bubble or upstream-condition dependency exists. The results are examined by means of POD analysis, and it turns out that the associated flow structures are largely identical to those expected from the swirl switching phenomenon.

METHODOLOGY and RESULTS

In the current simulations, the pipe consists of a part of a torus whose centre is located at the origin of the Cartesian system (X, Y, Z) . The toroidal coordinates (ζ, R, s) of the pipe and the local (in-plane) poloidal coordinates (r, θ) are illustrated in figure 1. The incompressible flow is expressed in Cartesian coordinates where the Navier–Stokes equations (NSE) read

$$\nabla \cdot \mathbf{u} = 0, \quad (1)$$

$$\frac{\partial \mathbf{u}}{\partial t} + (\mathbf{u} \cdot \nabla) \mathbf{u} = -\nabla p + \frac{1}{Re_b} \nabla^2 \mathbf{u}. \quad (2)$$

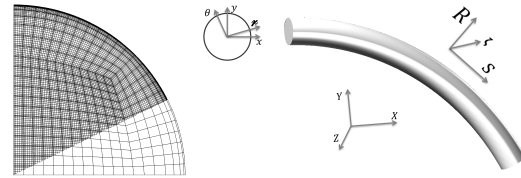


Figure 1. (Left) A quarter of a cross-sectional plane of the spectral-element pipe mesh. The Gauss–Lobatto–Legendre points are shown in the darker region. (Right) Cut-away view of toroidal pipe geometry and its associated Cartesian, plane poloidal and toroidal coordinate systems.

Here, \mathbf{u} indicates the velocity vector of the fluid flow in space (\mathbf{x}) and time (t), and p is the pressure. Dividing the physical domain into a number of hexahedral local elements, the incompressible NSE are solved by means of local approximations based on high-order orthogonal polynomial basis on the Gauss–Lobatto–Legendre (GLL) nodes. In this way the spectral accuracy with geometrical flexibility is provided which makes the method suitable for problems with moderately complex geometries. This spectral element method (SEM) has been developed and implemented by Fischer *et al.* (2008) as the massively parallel code `nek5000`.

The present simulations are carried out in a mildly curved pipe ($\kappa = 0.01$), a strongly curved pipe with $\kappa = 0.1$ and a full torus at $\kappa = 0.3$. The bulk Reynolds number is fixed to 11700 for all the simulations which ensures that the flow remains turbulent for all the cases. The numerical setup is similar to the one used by Noorani *et al.* (2013) for their highest Reynolds number; in particular the resolutions are the same. The mesh topology and pipe lengths ($L = 25R_a$) are also the same, except for the full torus which has the length of $L = 20.93R_a$. A quarter of the cross-sectional plane of the pipe mesh is shown in figure 1. The no-slip boundary condition is used for the walls and periodicity is applied for the end sections of the pipe domains in the axial direction since the flow is assumed to be homogeneous in this direction. The laminar Poiseuille profile of the straight pipe is used as the initial condition for all the simulations. After this initialisation the flow is perturbed with low-amplitude pseudo-random noise. While the mass flux is fixed, these simulations are evolved in time until the turbulent state is statistically fully developed in the pipe (around $200u_b/R_a$ from the start). Validation of the method and verification of the computation of turbulent statistics via tensor rotation from Cartesian system to toroidal/poloidal coordinates is conducted by Noorani *et al.* (2013).

From the instantaneous cross-sectional views of the axial velocity, shown in figure 2, it is obvious that with increasing κ the bulk flow is deflected more towards the outer bend of the curved pipes and the flow loses its azimuthal homogeneity which results in a sharp decrease of the turbulence activity in their inner side. The mean Dean vortices in these configurations are displayed in figure 3 by means of in-plane stream function.

In order to capture the dominant structures in the flow fields the POD of the DNS data is performed on the full domain. The POD modes are computed using the snapshot method (Sirovich, 1987). The approach is identical to POD analysis performed by Noorani & Schlatter (2015) in similar geometry at lower Re to analyse turbulent flow with sub-laminar drag in mildly curved pipes. The velocity field is interpolated from the SEM grid onto a poloidal grid with 128 slabs in the streamwise direction (s). Since the flow is fully developed, it is statistically stationary and homogeneous in s . The eigenfunctions of the POD, hence, are trigonometric in this direction, *i.e.* the j^{th} component of the velocity $u_j(\zeta, R, s)$ can be computed using the Fourier decomposition

$$u_j(\zeta, R, s) = \sum_k \hat{u}_j(\zeta, R, k) e^{i2\pi ks/L_s} \quad (3)$$

where Fourier coefficient $\hat{u}_j(\zeta, R, k)$ is a random function of the in-plane inhomogeneous directions (ζ, R) with parameter k . Then Karhunen–Loève expansion of these Fourier

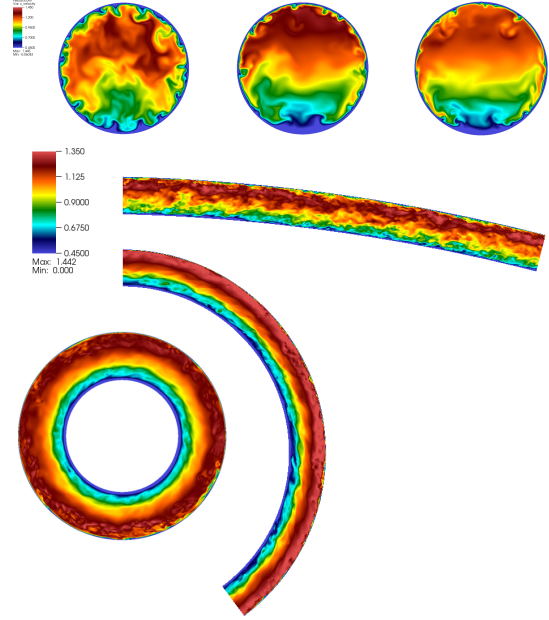


Figure 2. (Top) Pseudocolours of axial velocity in a cross-section of mildly and strongly curved pipes (*from left*: $\kappa = 0.01, 0.1$, and 0.3 as full torus); (Bottom) same quantity in the plane of symmetry of various curved configurations.

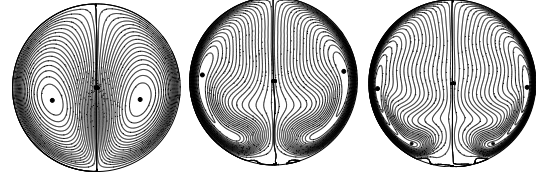


Figure 3. Iso-contours of mean cross-flow stream function Ψ for different curved configurations. (*from left*: $\kappa = 0.01, 0.1$, and 0.3)

coefficients is performed as

$$\hat{u}_j(\zeta, R, k) = \sum_m a_{j(m,k)} \phi_{(m,k)}(\zeta, R) \quad (4)$$

wherein the $\phi_{(m,k)}(\zeta, R)$ are the orthogonal basis functions (POD modes) and $a_{(m,k)}$ are the corresponding time-coefficients. No geometrical symmetries are considered for the in-plane components. The decomposition is performed with 1200 snapshots equidistantly distributed in time for 600 convective units. Hence $m \in (0, 1199)$ and $k \in (0, \pm 64)$, where the \pm represents the both real and imaginary part of the mode and the mean is represented by $\phi_{(0,0)}$ mode. The time frame of POD analysis and other relevant simulation parameters are listed in Table 1. Note that to reconstruct the velocity field, $\mathbf{u}(\mathbf{x}, t)$, a POD mode, $\phi_{(m,k)}(\mathbf{x})$, makes its contribution to the flow, $\mathbf{u}_{(m,k)}(\mathbf{x}, t)$, through two possible degeneracies as

$$\mathbf{u}_{(m,k)}(\mathbf{x}, t) = a_{(m,k)}(t) \phi_{(m,k)}(\mathbf{x}) + a_{(m,-k)}(t) \phi_{(m,-k)}(\mathbf{x}) \quad (5)$$

For brevity only the results of POD analysis in strongly curved pipe flows ($\kappa = 0.1$ and 0.3) will be shown here. The

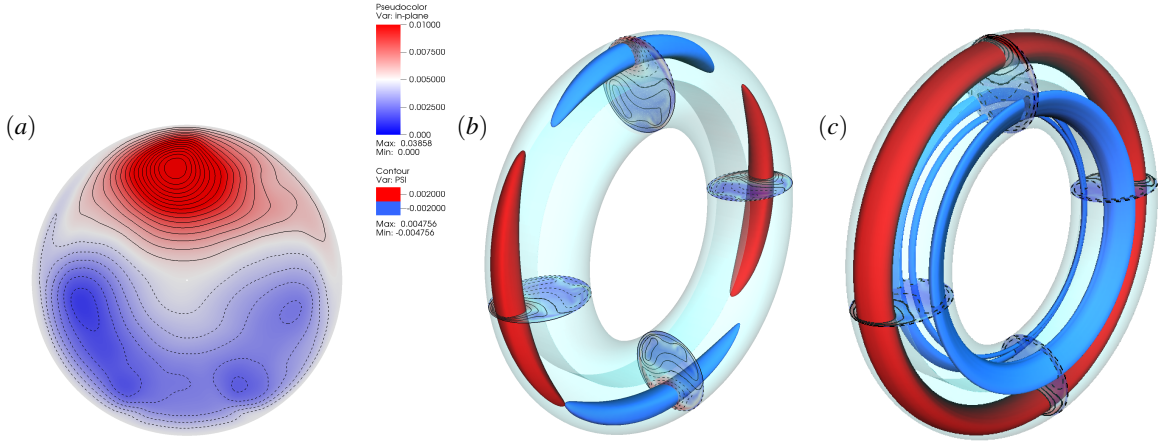


Figure 5. (a) A cross-sectional view of the in-plane stream function $\Psi_{(r,\theta)}$ of the most energetic POD mode $\phi_{(0,2)}$ for $\kappa = 0.3$ and $Re = 11700$. In order to emphasize the vortical structure of the mode, the positive and negative iso-values of Ψ are shown by solid and dashed lines projected on top of the pseudocolours of the same quantity. (b) Iso-surfaces of highly negative and positive values of Ψ from reconstruction of the POD mode $\phi_{(0,2)}$. The *red* surfaces are positive values, indicating the clockwise vortical motion, and the *blue* surfaces illustrate counter clockwise vortices. The pseudocolours of magnitude of the in-plane components $\sqrt{\langle u_r \rangle^2 + \langle u_\theta \rangle^2}$ are plotted in four cross-sectional planes of the pipe with in-plane isotachs of Ψ projected on top. On the slabs, positive and negative vortices are indicated with solid and dashed lines, respectively. (c) Similar to (b) but for $\phi_{(1,0)}$.

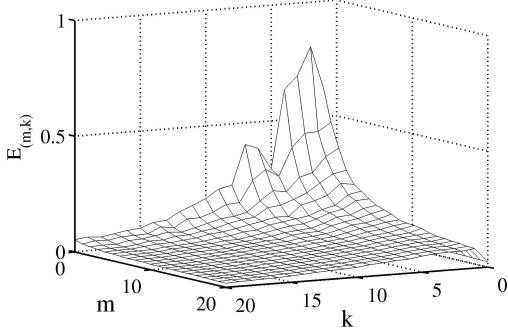


Figure 4. Eigenspectrum function of POD mode number (m) and streamwise wavenumber (k) for $m \in (0,20)$ and $k \in (0,\pm 20)$.

Table 1. Parameters of the present study. The non-dimensional friction Reynolds number Re_τ is defined as $\bar{u}_\tau R_a / \nu$; \bar{u}_τ is the azimuthally averaged mean friction velocity.

$Re_{b,D}$	κ	Re_τ	POD time frame (tu_b/R_a)
11700	0.01	368	600
11700	0.1	410	600
11700	0.3	470	600

energy content of various POD modes $E(m,k)$ of the turbulent flow in the full torus is shown in figure 4. Only the fluctuations part of the POD modes are shown in the figure to demonstrate how the main characteristics of the flow evolves. From the spectrum it is clear that large portion of

the energy of the fluctuations are shared amongst the group of modes $\phi_{(0,1-4)}$ and $\phi_{(1,1-4)}$. The energy of the modes $\phi_{(0,6-8)}$ also forms a second peak.

The most energetic POD mode for flow in the torus $\phi_{(0,2)}$, and some flow field reconstructions are shown in figure 5. Out of 3D velocity components, here the in-plane stream function is illustrated, particularly to emphasize the role of vortical structures in 2D, the sense of rotation and their evolutions. The mode shape in figure 5 (a) represents a family of modes governing the fluctuation part of the turbulence in bent pipes. This coherent structure essentially consists of two vortical cells with the much more dominant vortex having a support on the outer bend. The cell in the inner side is weaker and is a composite of smaller vortices. The mode is not completely symmetric with respect to the equatorial midplane of the pipe. The in-plane representation of this mode is very similar to the most energetic POD modes found by Kalpakli & Örlü (2013) and Carlsson (2014) close to a pipe-bend. Also the second most energetic POD mode in spatially developing 90° bends in Sakakibara *et al.* (2010), Hellström *et al.* (2013) and Kalpakli Vester *et al.* (2015) that is normally referred to as tilted Dean cells is very similar to the current structure.

Figure 5 (b) displays the flow reconstruction of this modes ($\phi_{(0,2)}$). The iso-surfaces of maximum/minimum in-plane stream function $\Psi_{(r,\theta)}$ are displayed in the figure to mark the core of the dominant vortex in the outer side of the curve, which switches the sign between negative (CW) and positive (CCW) values. The reconstruction of the sub-dominant mode $\phi_{(1,0)}$ is displayed in figure 5 (c). While this mode has the same in-plane shape as the most energetic family, it is essentially stationary and invariant in streamwise direction. The strength of vortices oscillate and switch the sign only in time.

The temporal behaviour of the modes $\phi_{(0,\pm 2)}$ and $\phi_{(0,\pm 1)}$ are illustrated in figure 6. The sinusoidal behaviour of $\phi_{(0,\pm 2)}$ is obvious from their time coefficients (figure 6 a). The quasi-periodic nature of these family of modes

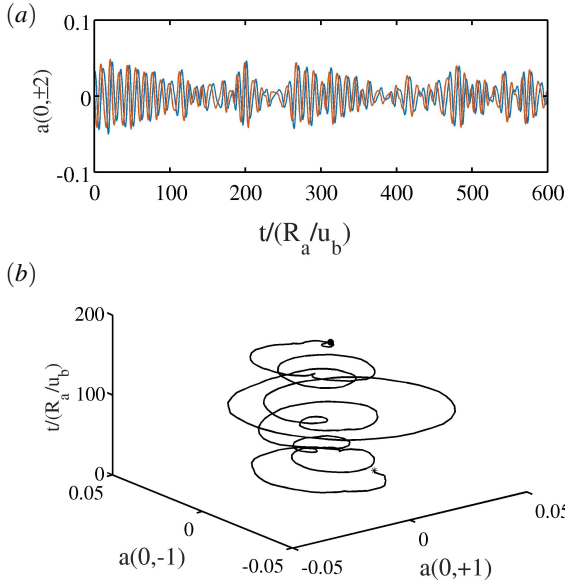


Figure 6. (a) The temporal behaviour of the POD mode $\phi_{(0,\pm 2)}$ in torus (— $+k$ and — $-k$). (b) The temporal orbit of the time coefficients of the mode $\phi_{(0,\pm 1)}$ in torus. Only the first $175tu_b/R_a$ is shown where * and • represent the beginning and the end of the trajectory.

is emphasized illustrating the temporal orbit of the mode $\phi_{(0,\pm 1)}$ in the figure 6 (b). This figure displays how the mode wobbles and jumps between different frequencies propagating in time.

The PSD analysis of the time coefficient of the most energetic group of modes for the torus case are presented in figure 7 (a). It is shown that the spatial higher harmonics of the mode $\phi_{(0,\pm 1)}$ are also higher harmonics of this mode in time. Figure 7 (b) displays the PSD of the time coefficients of the other energetic modes in comparison to the mode $\phi_{(0,\pm 1)}$. It is quite clear that almost all the low wave number energetic POD modes are oscillating with two dominant frequencies of $St \approx 0.01$ and $St \approx 0.09$ and their higher harmonics.

Similar to figure 5, an in-plane cut of the most energetic structure in turbulent flow with $\kappa = 0.1$ ($\phi_{(0,2)}$) and a snapshot of its reconstruction is shown in figure 8. The mode-shape in this flow configuration is quite similar to that of the torus case. The reconstruction of the mode (figure 8 b) indicates that the switching between CW and CCW states is not abrupt, and the mode is transitional in both space and time. While the strength of these vortices oscillates in time (and also in streamwise direction) these cells interchange energy and the two dominant cells change the sign correspondingly. Half-way through their period they are weakened and the inner-bend structure is torn apart. One of the resulting cells is pushed towards the outer bend and become the dominant vortex, but now with the opposite sign. A sub-dominant mode in this geometry ($\phi_{(1,0)}$) is also invariant in the streamwise direction and only oscillating in time with very low frequencies. The in-plane shape of this mode is also very similar to what is referred as tilted Dean cells in the literature. These data accentuate the similarity of the dominant structures in the strongly curved pipes with different curvature.

Figure 9 provides a direct comparison of the flow reconstruction of the most energetic POD modes and the

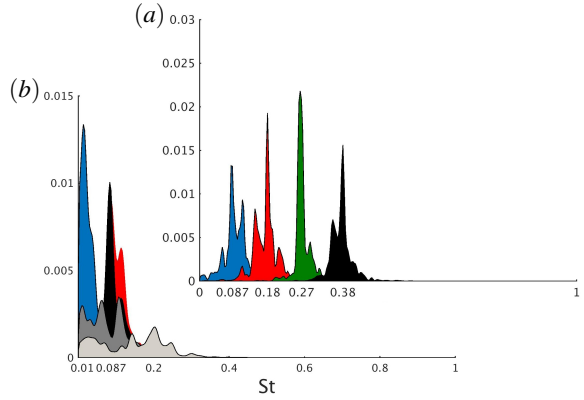


Figure 7. Welch's estimation of the power spectral density of time coefficients of different families of POD modes in torus (a) with 50% window and 25% overlap; (blue) $\phi_{(0,1)}$; (red) $\phi_{(0,2)}$; (green) $\phi_{(0,3)}$; (black) $\phi_{(0,4)}$. (b) with 25% window and 12% overlap; (blue) $\phi_{(1,0)}$; (red) $\phi_{(0,1)}$; (black) $\phi_{(1,1)}$; (dark-gray) $\phi_{(2,1)}$; (light-gray) $\phi_{(3,1)}$.

mean flow computed from a stereo-PIV in a 90° bend by Kalpakli & Örlü (2013) with the present DNS data. The POD reconstruction of DNS data (for both $\kappa = 0.1$ and 0.3) is performed using the mean and the most energetic family of modes ($\phi_{(0,1-9)}$). It is quite clear that similar to turbulent flow through 90° pipe-bends, in the current toroidal pipes also the alternating domination of Dean cells (swirl switching) exists. Surprisingly, no single swirl mode similar to what previously identified in the POD analysis of turbulent flow in spatially developing bends is found among the most energetic groups in the current study. The significance of the current results lies in the fact that the swirl switching mechanism is observed in a toroidal pipe where there is no separation or upstream dependency exists. This in itself indicates that the swirl switching might essentially be the effect of the curvature rather than other proposed mechanisms.

CONCLUSIONS

Proper orthogonal decomposition of DNS data of turbulent flow in strongly curved toroidal pipes at $Re = 11700$ is performed. The most energetic structures are divided into multiple groups according to their streamwise wavenumber and energy content. It is shown that the mode shape of the most energetic group is very similar for flow in different curvature configurations $\kappa = 0.1$ and 0.3 . This mode, which oscillates in time with very low frequencies, resembles the dominant structure identified for turbulent flow in 90° bends commonly referred to as tilted Dean cells. The flow field reconstruction with energetic modes and mean flow represents the alternating domination of the Dean cells which confirms the existing of swirl switching mechanism in toroidal pipes. Despite the existence of swirl switching in these configurations, the single-vortex mode (so-called the switch mode) previously observed in the pipe-bend literature is not appeared in the current analysis. The existence of swirl switching in toroidal pipes brings up the idea that this phenomenon might be due to the effect of the curvature itself.

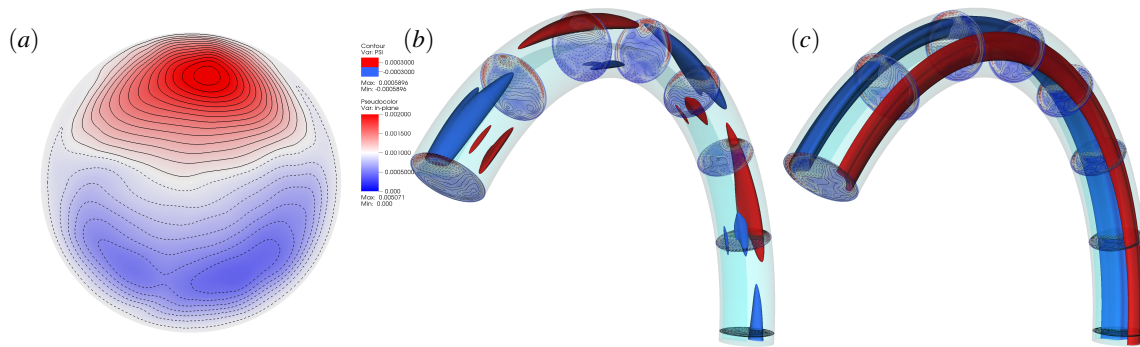


Figure 8. Similar to figure 5 but in turbulent curved pipe with $\kappa = 0.1$ and $Re = 11700$.

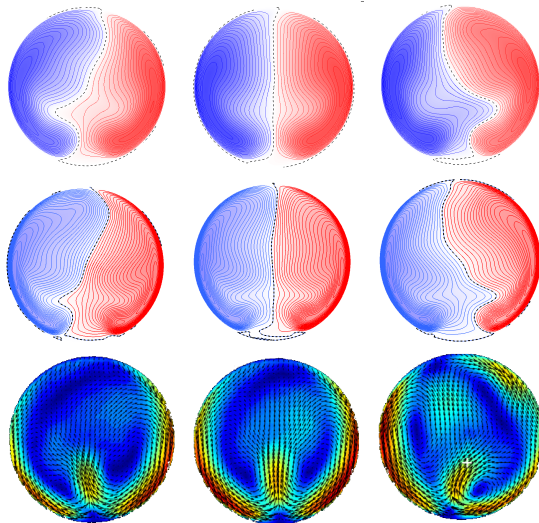


Figure 9. Three typical time instances of reconstructed flow field from the most energetic POD modes and the mean, for strongly curved pipe with $Re = 11700$, $\kappa = 0.1$ (top); torus with $Re = 11700$, $\kappa = 0.3$ (middle); and for an experiment in a spatially developing 90° bend at $Re = 34000$ and $\kappa = 0.36$ (bottom). Reprinted from Kalpakli & Örlü (2013). (Top panels) Iso-contours of stream function Ψ projected on top of its pseudocolours where red represents positive and blue indicates negative values of Ψ . (Bottom) Pseudocolours of magnitude of the in-plane components with arrows indicating in-plane velocity.

ACKNOWLEDGEMENT

The authors wish to acknowledge Drs. Athanasia Kalpakli Vester and Ramis Örlü for fruitful discussions and providing the experimental data. Funding from Swedish e-Science Research Centre (SeRC) and computer time that was provided by the Swedish National Infrastructure for Computing (SNIC) is acknowledged.

REFERENCES

Brücker, C. 1998 A time-recording DPIV-study of the swirl switching effect in a 90° bend flow. In *Proceedings of the*

Eight International Symposium on Flow Visualization, 1-4 September, Sorrento, Italy.

- Carlsson, Ch. 2014 Utilization of decomposition techniques for analyzing and characterizing flows; paper 1. swirl switching in turbulent flow through 90° pipe bends. PhD thesis, Division of Fluid Mechanics, Department of Energy Sciences, Lund University, Sweden.
- Fischer, P. F., Lottes, J. W. & Kerkemeier, S. G. 2008 <http://nek5000.mcs.anl.gov>.
- Hellström, L.H.O., Zlatinov, M.B., Cao, G. & Smits, A.J. 2013 Turbulent pipe flow downstream of a bend. *J. Fluid Mech.* **735**, R71–12.
- Kalpakli, A. & Örlü, R. 2013 Turbulent pipe flow downstream a 90° pipe bend with and without superimposed swirl. *Int. J. Heat Fluid Flow* **41**, 103–111.
- Kalpakli Vester, A., Örlü, R. & Alfredsson, P. H. 2015 POD analysis of the turbulent flow downstream a mild and sharp bend. *Exp. Fluids* **56** (3), 1–15.
- Kim, K.C. & Adrian, R.J. 1999 Very large-scale motion in the outer layer. *Phys. Fluids* **11** (2), 417–422.
- Noorani, A., El Khoury, G.K. & Schlatter, P. 2013 Evolution of turbulence characteristics from straight to curved pipes. *Int. J. Heat Fluid Flow* **41**, 16–26.
- Noorani, A. & Schlatter, P. 2015 Evidence of sublamina drag naturally occurring in a curved pipe. *Phys. Fluids* **27** (3), 035105.
- Rütten, F., Meinke, M. & Schröder, W. 2001 Large-eddy simulations of 90° degrees pipe bend flows. *J. Turb.* **2**, 1–14.
- Rütten, F., Schröder, W. & Meinke, M. 2005 Large-eddy simulation of low frequency oscillations of the Dean vortices in turbulent pipe bend flows. *Phys. Fluids* **17** (3), 035107.
- Sakakibara, J. & Machida, N. 2012 Measurement of turbulent flow upstream and downstream of a circular pipe bend. *Phys. Fluids* **24** (4), 041702.
- Sakakibara, J., Sonobe, R., Goto, H., Tezuka, H., Tada, H. & Tezuka, K. 2010 Stereo-PIV study of turbulent flow downstream of a bend in a round pipe. *14th Int. Symp. Flow Vis. EXCO Daegu Korea*.
- Sirovich, L. 1987 Turbulence and the dynamic of coherent structures, part 1–3. *Quart. App. Math.* **45**, 516–590.
- Tunstall, M.J. & Harvey, J.K. 1968 On the effect of a sharp bend in a fully developed turbulent pipe-flow. *J. Fluid Mech.* **34** (03), 595–608.